Journal of Applied Electrochemistry **30**: 1389–1395, 2000.

Electrochemical oxidation of carbon in a 62/38 mol % Li/K carbonate melt†

W.H.A. PEELEN, M. OLIVRY, S.F. AU, J.D. FEHRIBACH‡ and K. HEMMES*
Delft University of Technology, Faculty of Applied Sciences, Laboratory for Material Science, Rotterdamseweg 137, 2628 AL Delft, The Netherlands
*(*author for correspondence, e-mail: K.Hemmes@tnw.tudelft.nl)*

Received 31 July 1999; accepted in revised form 14 December 1999

Key words: carbon, coal, electrochemical oxidation, fuel cells

Abstract

The electrochemical gasification of coal to CO in a direct carbon fuel cell (DCFC) has thermodynamical advantages, including the conversion of heat into power at a reversible efficiency of 100%. Molten carbonate fuel cell (MCFC) technology may form the basis for constructing DCFC's. Here the electrochemical oxidation of carbon in a 62/38 mol % Li/K carbonate melt is studied using impedance spectroscopy (IS) and cyclic voltammetry (CV). A set of equilibria is introduced which fully describes the electrochemical equilibrium of the system. From IS it is shown that for temperatures lower than 700 °C, charge transfer is the slowest step, while at higher temperatures a second unidentified step also contributes significantly to the d.c. resistance of the electrode. The d.c. resistance is 100 to 220 Ω cm^2 at 650 °C and 12 to 60 Ω cm^2 at 750 °C, depending on the carbon surface roughness.

1. Introduction

As the worldwide demand for energy continues to increase over the next fifty years, the portion of this demand met by oil, gas and uranium will begin to decline. It is not certain that the development of such long-term alternatives as solar, water, wind, fusion or biomass will be sufficiently in line to compensate for this decline. The world must therefore search for intermediate-term sources. One obvious possibility is coal; it is abundant and cheap, albeit currently heavily polluting. Since future environmental requirements will be strict, clean coal conversion techniques are needed.

A number of studies have dealt with coal conversion techniques [1–6]. One promising possibility is the direct electrochemical conversion of coal to CO,

$$C(s) + \tfrac{1}{2}\,O_2(g) \leftrightarrow CO(g) \qquad (1)$$

in a direct carbon fuel cell (DCFC) [7, 8] (throughout this work, coal is synonymous with solid carbon: C(s)). These cells circumvent the gasification/combustion steps of present processes and have an advantage over other fuel cells in that a reversible efficiency greater than unity can be obtained [9, 10]. Furthermore the CO produced can be utilized in the form of syngas. Early attempts to employ coal in a fuel cell were reported by Becquerel [10], but at this time only two studies have directly considered the development of a DCFC [7, 8]. This lack of interest is probably due to the carbon oxidation rates, which are generally known to be small, and to difficulties in constructing a fuel cell that operates on a solid fuel instead of much more conventional gaseous and liquid fuels. However, some alkali metal salts, especially lithium carbonate, are reported to have a catalytic effect on the gasification of carbon [11–14]. This opens up the possibility of developing DCFCs based on existing molten carbonate fuel cell (MCFC) technology. One study by Vutetakis and Skidmore [13] explicitly deals with the electrochemical oxidation of different coal/carbon slurries in the Li/Na/K carbonate eutectic under CO_2 for temperatures between 500 °C and 800 °C. But the emphasis was on obtaining large rates for the electrochemical conversion of C to CO_2 instead of to CO.

Obviously a fundamental understanding of carbon oxidation in molten carbonate is helpful when attempting to increase the rate of oxidation to CO. Therefore, this work begins with a theoretical description of the electrochemical system consisting of carbon immersed in molten carbonate under a CO_2/CO gas atmosphere. This is followed by an impedance spectroscopy (IS) and cyclic voltammetry (CV) study of carbon oxidation in a 62/38 mol % Li/K carbonate melt as a function of temperature under a 100% CO_2 gas atmosphere.

† Dedicated to the memory of Daniel Simonsson
‡ On leave from WPI Mathematical Sci., 100 Institute Rd, Worcester, MA 01609 USA

2. Experimental details

The half-cell set-up used here was as described previously [15]. The only change was the working electrode. Here it consisted of a graphite rod (Alfa), 2 cm long by 6.5 mm diameter, rigidly connected to an alumina tube using a high-temperature cement (Gimex, type 503) and a gold screw (Figure 1). A gold wire, shielded from the carbonate melt by the alumina tube, was used as electrical lead out of the cell. To avoid contact between the melt and the carbon/alumina junction (and thus possible leakage), only 1 cm of the carbon was immersed in the melt. An immersed surface area of 2.04 cm^2 was obtained. Visual inspection showed that there was little wetting of carbon by molten carbonate. This prevented the formation of a large meniscus at the electrode, and thus also prevented the large increase in the electrode surface area associated with this meniscus.

All the sweep voltammetry measurements were performed with an ECO Chemie potentiostat (PGSTAT20), using the GPES3 software package. The impedance measurements were performed with a Zahner Impedance unit (model IM6-12057). Impedance spectra were measured in the range between 5 mHz and 100 kHz, with a 10 step/decade and four single-frequency cycles averaged for each frequency. The impedance data were fitted using the Equivcrt Software package written by B.A Boukamp.

A well-defined measurement procedure was followed precisely in all experiments in order to eliminate, as much as possible, systematical errors. At the beginning of each experiment, the cell was always flushed with 100% CO_2. Then a new carbon electrode was lowered into the melt, and after obtaining a stable open cell potential (OCP) (typically 1 h later), impedance measurements were recorded at overpotentials of 0, 25, 50, 100, 150, 200, 300 and 400 mV. After the last impedance measurement, a sweep voltammetry measurement was recorded at a scan rate of 1 mV s^{-1} using a voltage range from OCP to typically −0.2 V relative to the standard oxygen reference (SOR) [16]. The electrode was left in the melt overnight, and the same procedure was repeated. In all, these experiment were performed on a total of eight carbon electrodes, three at 650 °C and 700 °C, and two at 750 °C.

3. Theory

To obtain a good understanding of the (electro)chemistry in our system, we described it using a complete and independent base set of equilibria as introduced by Smith and Missen [16] and Coleman and White [17]. This method was applied to molten carbonate systems earlier by Hemmes et al. [18]. For a DCFC, the species at the anode are carbonate ions, oxide ions, carbon, CO and CO_2, and the base set of (electro)chemical equilibria is then

$$CO_3^{2-} \leftrightarrow O^{2-} + CO_2 \tag{2}$$

$$C + 2\,CO_3^{2-} \leftrightarrow 3\,CO_2 + 4\,e^- \tag{3}$$

$$C + CO_3^{2-} \leftrightarrow CO + CO_2 + 2\,e^- \tag{4}$$

Equation 2 is the well-known dissociation/recombination equilibrium that is always present in molten carbonate. Equations 3 and 4 constitute the electrochemical oxidation of carbon to CO_2 and CO, respectively. Any other conceivable equilibrium in this system is obtained by a linear combination of equilibria Equations 2–4. For example, the well-known Boudouard equilibrium is obtained by subtracting twice Equation 4 from Equation 3:

$$CO_2 + C \leftrightarrow 2\,CO \quad K_B = \frac{(P_{CO})^2}{P_{CO_2} a_C} \tag{5}$$

For a DCFC using molten carbonate as its electrolyte, the cathodic process is oxygen reduction according to

$$2\,CO_2 + O_2 + 4\,e^- \leftrightarrow 2\,CO_3^{2-} \tag{6}$$

Combining the anodic and cathodic reactions (Equations 3, 4 and 6), the overall DCFC cell reactions (considering only CO_2 or CO production) are, respectively,

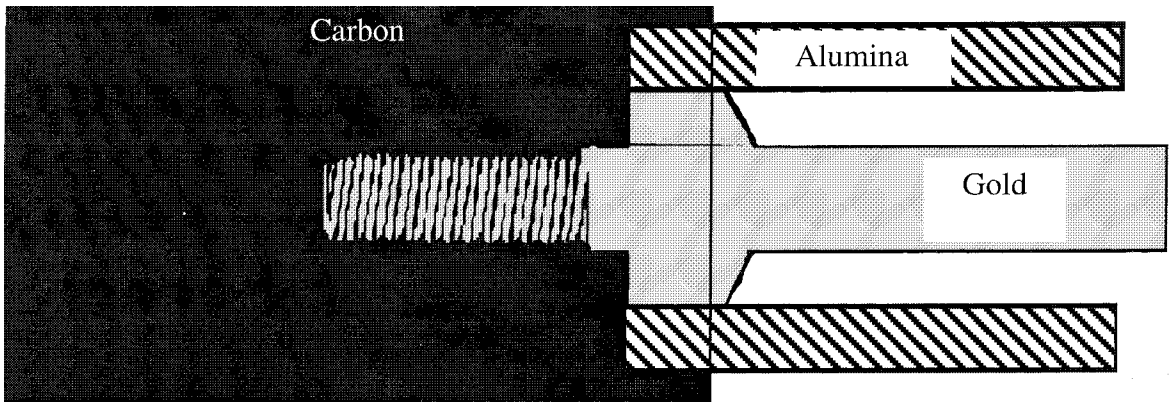

Fig. 1. Schematic representation of the carbon working electrode assembly.

$$C + O_2 \leftrightarrow CO_2 \quad (7)$$

$$C + \tfrac{1}{2}O_2 \leftrightarrow CO \quad (8)$$

In practice both processes can occur, depending on the applied electrode potential, the temperature and the kinetics of Reactions 3 and 4. For reasons explained elsewhere, CO_2 formation is less favoured compared to that of CO in a DCFC [9]. The distinction as to whether CO or CO_2 is formed can in principle be resolved thermodynamically by considering their respective standard potentials $E°$; these are listed for different temperatures in Table 1. In the temperature region of the MCFC, that is, near 923 K, the difference in $E°$ for both processes is rather low, less than 40 mV. Alternatively this difference can be expressed by the value of the Boudouard equilibrium constant K_B. The equilibrium partial pressures of CO and CO_2 can be calculated using Equation 5 (assuming $a_C = 1$) and $P_{CO} + P_{CO_2} = 1$ atm. From this calculation, one finds that for 900 K, both P_{CO} and P_{CO_2} are substantial, but for higher temperatures, CO is preferred thermodynamically over CO_2. If and to what extent CO and CO_2 are actually formed depends on the kinetics of the reactions involved, and these are unknown.

4. Results and discussion

4.1. *Voltammetry*

Figure 2 displays the I/V curves for a gold and graphite electrode under 1 atm of CO_2. At both electrodes, current increases exponentially with increasing potential. It is known that at the gold electrode this increase is caused by the oxidation of carbonate ions according to Equation 6 [19]. Since carbonate ions are present in excess, diffusion is not rate-limiting, that is, no current saturation is seen. The same behaviour with comparable current densities is seen for the carbon electrode, but at a much more negative potential of −0.6 V. Carbon is the only species present in sufficient amounts to give currents comparable to that in the carbonate oxidation. Similar results were found by Vutetakis and Skidmore when they added coal slurries to Li/K/Na carbonate [13]. Consequently the cyclic voltammograms recorded at the carbon electrode shown in Figure 3 reflect the carbon oxidation. Only one anodic wave is observed, and therefore no distinguishing information is obtained as to whether carbon oxidation results in CO, CO_2, or a mixture of both. The measured current density does not depend on scan rate, and is therefore not diffusion-limited, suggesting that charge transfer is the rate-determining step in the electrode process.

The reverse cathodic wave is peak shaped, with a peak potential proportional to the square root of the scan rate. A corresponding anodic peak is not seen. Both features indicate that this electrode process is irreversible. If the scan is first in cathodic direction, the peak is still present though at lower current densities. Therefore the cathodic wave must be due to a species initially present in the melt, but also directly or indirectly formed by carbon oxidation. Initially carbonate ions, oxide

Table 1. $E°(CO_2)$ and $E°(CO)$ for CO_2 (Equation 5) and CO (Equation 6) formation, respectively, the Boudouard constant K_B and the equilibrium CO and CO_2 pressures, as function of temperature

T/K	$E°$(CO)/V	$E°(CO_2)$/V	K_B/atm	$P^{eq}_{CO_2}$/atm	$P^{eq}_{CO_2}$/atm
800	−0.95	−1.03	0.01	0.91	0.09
900	−0.99	−1.03	0.16	0.67	0.33
1000	−1.04	−1.03	1.96	0.27	0.73
1100	−1.08	−1.03	29.2	0.03	0.97
1200	−1.13	−1.03	400	0.02	0.98

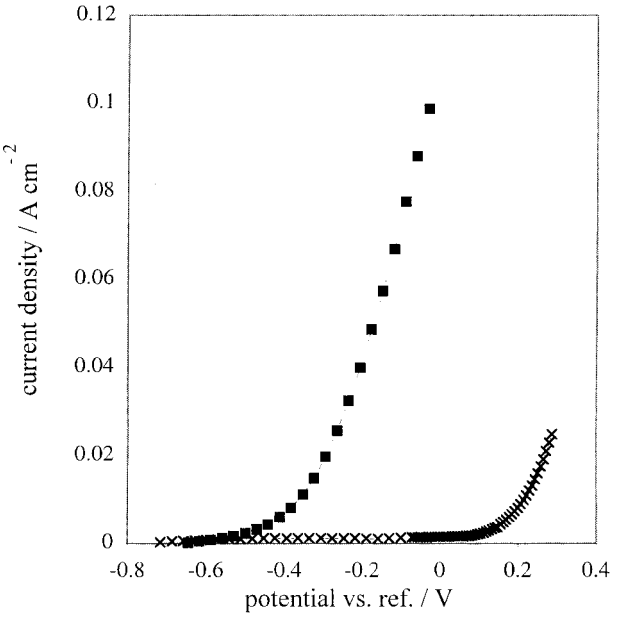

Fig. 2. Steady state polarization curves at 1 mV s^{-1} of a gold (×) and carbon (■) electrode at 650 °C under 1 atm CO_2.

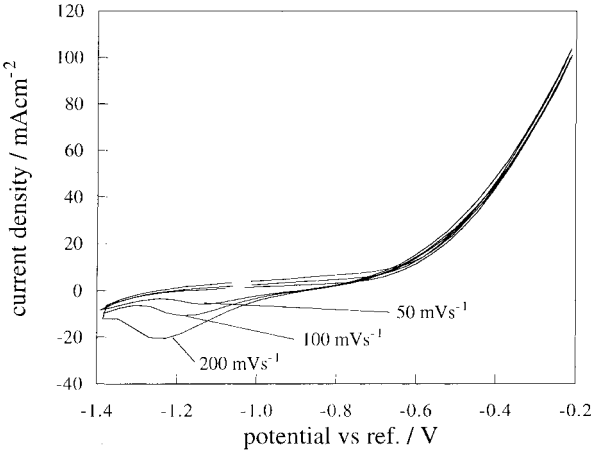

Fig. 3. Cyclic voltammograms starting in anodic direction at different scan rates of a carbon electrode at 650 °C under 1 atm CO_2.

ions, carbon, CO_2 and CO formed in the Boudouard reaction are present in the melt. From these species only CO and CO_2 can be reduced. Since CO solubility in the melt is known to be low [20], it is more likely that CO_2 is the species reduced in the cathodic wave, and hence also produced by carbon oxidation. This result agrees with those of Dunks [12] and Vutetakis and Skidmore [13] who also report that CO_2 is the main product in carbon oxidation in molten salts.

Figure 4 shows the temperature dependence of the carbon oxidation currents. Measured steady-state voltammograms for three different temperatures are shown, both for the new electrodes and those immersed for 24 h. Except at 750 °C, larger currents are obtained from electrodes immersed for 24 h. Also in each case, current increases with temperature, doubling from 650 to 700 °C and tripling from 700 to 750 °C.

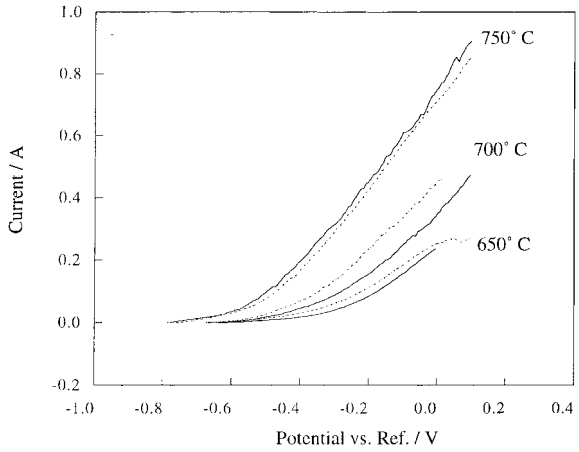

Fig. 4. Steady state voltammograms at a new carbon electrode at 650, 700 and 750 °C under 1 atm CO_2 with 1 mV s^{-1}. Key: (——) new electrode; (- - - -) immersed for 24 h.

4.2. *Impedance spectroscopy*

Figures 5, 6 and 7 show typical impedance spectra measured at temperatures of 650, 700 and 750 °C, respectively. For each temperature, measurements obtained for both new and immersed electrodes are depicted for overpotentials of 0 and 150 mV. All spectra have the following three features: At higher frequencies, a small arc is observed which is enlarged in Figure 8. It stems from stray capacitance in the lead wires and is not considered to be an electrode process. At intermediate frequencies of roughly 5 to 200 Hz, a large semicircular arc is observed. Finally, at lower frequencies, a smaller second arc is present. Its shape is ill-defined at frequencies lower than 0.5 Hz due to a large scatter in the measured data.

To quantify these findings, a simple Randles circuit was fitted to the large semi-circular arc seen at intermediate frequencies using a 0 mV overpotential. The frequencies used in the fit were chosen separately for each spectrum to obtain the best possible fit, but were typically in the range 5–200 Hz. The values for the uncompensated electrolyte resistance R_E, the charge transfer resistance R_{CT}, and the double layer capacitance C_{DL} resulting from the least square fit of the Randles circuit are listed in Table 2. The fit results obtained for R_{CT} and C_{DL} were, respectively, multiplied and divided by the geometric surface area to obtain what we call specific values. Also listed in Table 2 are the values for the specific d.c. resistance of the electrode which is represented by the width of the measured IS spectrum multiplied with the geometric surface area. From anodic steady-state measurement, Nekrasov et al. determined a polarization resistance of a spectral graphite electrode under CO_2 in NaCl-KCl–(Na_2CO_3 1%) at 780 °C of 23 Ω cm^2 [21]. This value is on the same order of magnitude as the electrode resistances obtained here in a Li/K carbonate melt at 750 °C. These values for the carbon oxidation are very low, for

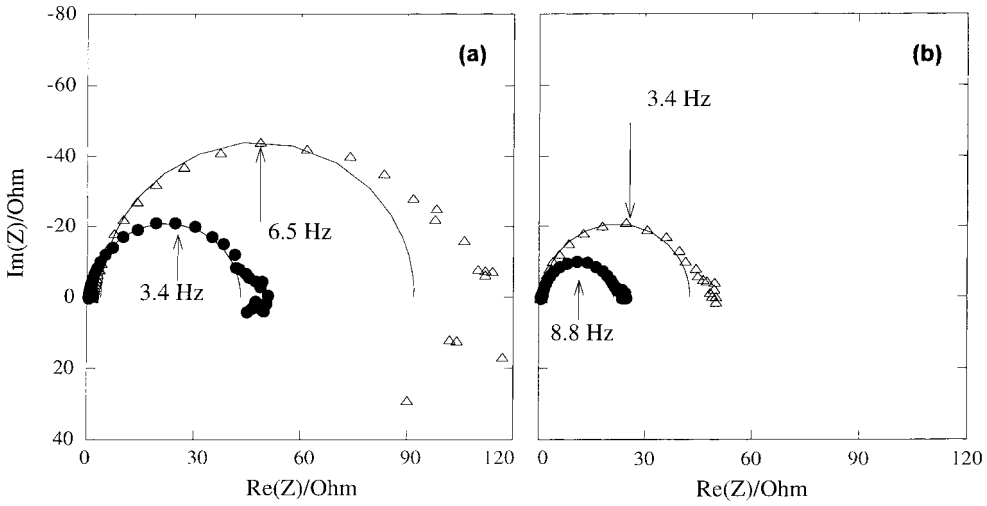

Fig. 5. IS spectra at a new carbon electrode (a) and one immersed for 24 h (b) in a Li/K melt at 650 °C under 1 atm CO_2 at $\eta = 0$ (△) and 150 mV (●) and the fitted Randles circuit (solid line).

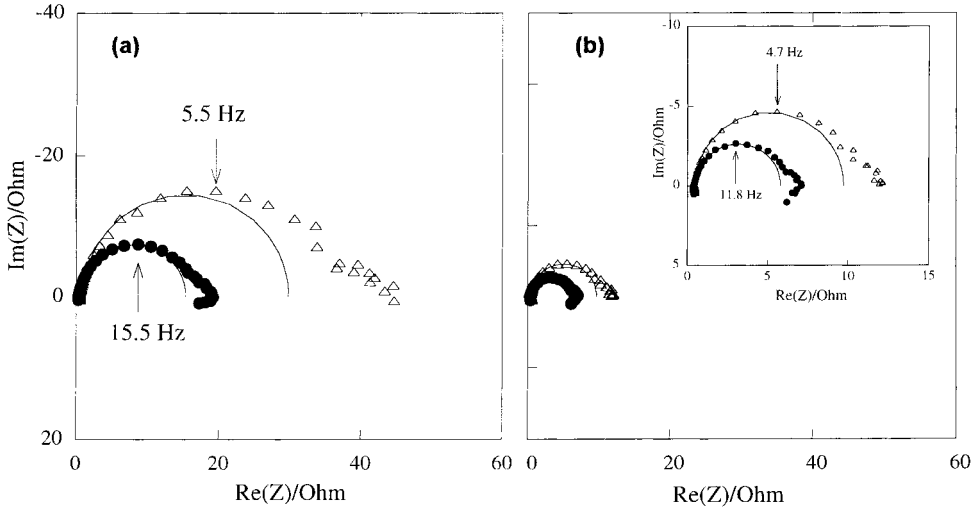

Fig. 6. IS spectra at a new carbon electrode (a) and one immersed for 24 h (b) in a Li/K melt at 700 °C under 1 atm CO_2 at $\eta = 0$ (△) and 150 mV (●) and the fitted Randles circuit (solid line). Inset is an enlargement of the same plot.

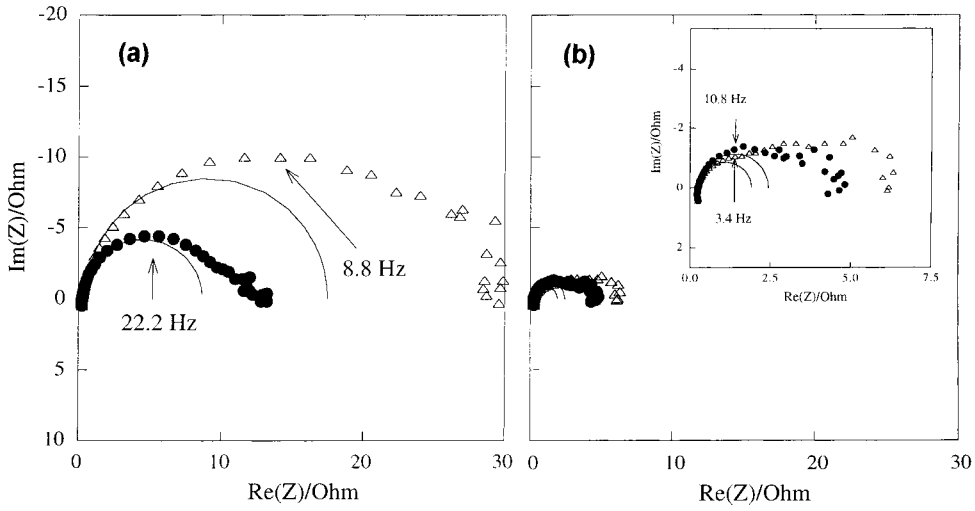

Fig. 7. IS spectra at a new carbon electrode (a) and one immersed for 24 h (b) in a Li/K melt at 750 °C under 1 atm CO_2 at $\eta = 0$ (△) and 150 mV (●) and the fitted Randles circuit (solid line). Inset is an enlargement of the same plot.

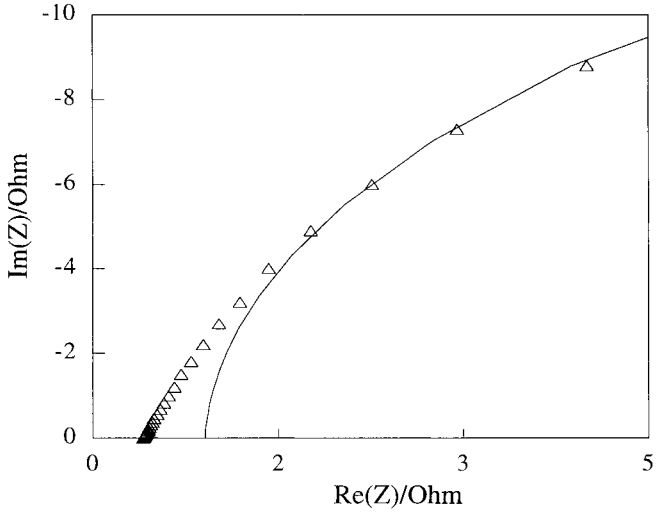

Fig. 8. IS spectrum for 500 Hz and 100 kHz of a new carbon electrode in a Li/K melt at 700 °C under 1 atm CO_2 at $\eta = 0$ and the fitted Randles circuit (solid line).

example, the charge transfer resistance for the H_2 oxidation under standard anodic MCFC gas at 650 °C at a nickel flag electrode is 0.13 Ω cm^2 [22].

In Figures 5, 6 and 7 and Table 2, the effect of the immersion time on the IS response is clearly observable. R_{CT} decreases by a factor 2 at 650 °C, a factor 3 at 700 °C and a factor 10 at 750 °C after 24 h of immersion. These factors correlate nicely with the increase in the double layer capacitance which increases in roughly the same way. This shows that the decrease in R_{CT} is most probably due to an increase in the electroactive surface area.

The nature of the small low frequency arc remains unresolved here. Its effect on the oxidation rate is quantified in Figure 9 where the ratio of R_{CT} and R_{DC} for the new electrode and the one immersed for 24 h are plotted as function of temperature. Though the error margins in the plot are large, it shows that the relative importance of the second arc to R_{DC} increases with

Table 2. R_{DC}, R_E, R_{CT} and C_{DL}, determined with impedance spectroscopy at a new electrode and at one immersed in the melt for 24 h

T/°C	New electrode				Immersed for 24 h			
	$R_{DC}/\Omega\ cm^2$	R_E/Ω	$C_{DL}/mF\ cm^{-2}$	$R_{CT}/\Omega\ cm^2$	$R_{DC}/\Omega\ cm^2$	R_E/Ω	$C_{DL}/mF\ cm^{-2}$	$R_{CT}/\Omega\ cm^2$
650	220 ± 20	1.4 ± 0.2	0.16 ± 0.01	170 ± 20	100 ± 10	1.3 ± 0.2	0.30 ± 0.05	80 ± 7
700	110 ± 5	1.0 ± 0.2	0.4 ± 0.05	55 ± 4	24 ± 2	0.5 ± 0.1	1.5 ± 0.1	18 ± 2
750	60 ± 5	0.5 ± 0.1	0.2 ± 0.05	35 ± 2	12 ± 2	0.3 ± 0.1	2.9 ± 0.2	3 ± 0.5

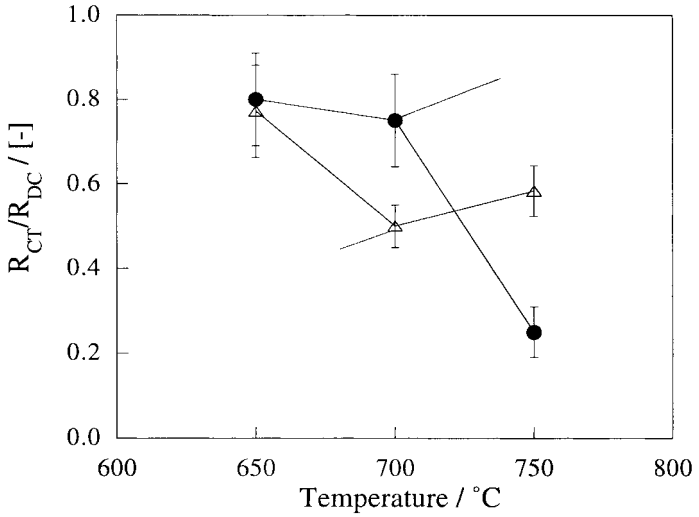

Fig. 9. Ratio of R_{CT} and R_{DC} as function of temperature for a new electrode (△) and one immersed for 24 h (●). Solid lines drawn to guide the eye.

temperature. For an electrode immersed for 24 h at 750 °C the resistance stemming from the low frequency process is 75% of the d.c. resistance. Assuming that the large semicircle is due the oxidation of C to CO_2, it is tempting to conclude that the low frequency circle is due to C oxidation to CO. This conclusion seems even more reasonable since at high temperature the Boudouard equilibrium prefers CO over CO_2 as shown in Table 1. However, with this second oxidation, an additional, parallel reaction path is obtained. Hence a decrease in R_{DC} must then be expected compared to R_{DC} when only determined by the C oxidation to CO_2. The IS spectra, however, clearly show that the second arc increases the d.c. electrode resistance. It is therefore more likely that the second arc stems from a homogeneous reaction in which the Boudouard reaction or CO is involved.

The above IS results show clearly that when targeting for improved carbon oxidation rates at temperatures of 750 °C and higher, one should initially focus on accelerating the process giving rise to the low frequency arc and not (only) on accelerating charge transfer.

5. Conclusions

The oxidation of carbon in molten carbonate is a slow process. The d.c. electrode resistance R_{DC} (100 to 220 $\Omega\ cm^2$) is largely determined by the charge transfer resistance and is about three orders of magnitude higher than that obtained for the hydrogen oxidation at a nickel electrode at 650 °C in the same melt. For temperatures lower than 700 °C, the rate limiting process is a charge transfer resistance R_{CT}. For higher temperatures, an additional unidentified process also contributes considerably to R_{DC}. The R_{DC}, C_{DL} as well as the R_{CT} decrease with immersion time due to surface roughening, until after 24 h a stable electrode is obtained. When temperature is varied, R_{CT} decreases by a factor of 5 for a newly immersed electrode when going from 650 °C to 750 °C, while for an electrode immersed for 24 h, this factor is 25. For R_{DC} these changes are by factors of 4 and 8, respectively.

Acknowledgements

NEDO is acknowledged for its financial support in the programme AE3 FY96.97.98 'Design and optimization of porous electrodes and advanced material developments'.

References

1. R.W. Coughlin and M. Farooque, *Nature* **279** (1979) 301–303.
2. R.W. Coughlin and M. Farooque, *J. Appl. Electrochem.* **10** (1980) 729–40.
3. R.W. Coughlin and M. Farooque, *Ind. Eng. Chem. Process Des. Dev.* **19** (1980) 211–19.
4. R.W. Coughlin and G. Kreysa, *Int. Chem. Eng.* **24** (1984) 585.

5. M. Farooque, A. Kush, H. Maru and J. MacDonald, *J. Appl. Electrochem.* **21** (1991) 143–50.
6. G. Thomas, M. Chettiar and V.I. Birss, *J. Appl. Electrochem.* **20** (1990) 941–50.
7. N. Nakagawa and M. Ishida, *Ind. Eng. Chem. Res.* **27** (1988) 1181–1185.
8. T. Horita, N. Sakai, T. Kawada, H. Yokokawa and M. Dokiya, *J. Electrochem. Soc.* **142** (1995) 2621–24.
9. W.H.A. Peelen, K. Hemmes and J.H.W. de Wit, *High Temp. Mater. Process.* **2** (1998) 471–82.
10. J.A.A. Ketelaar, *in* L.J.M.J. Blomen and M.N. Mugerwa (Eds), 'Fuel Cell Systems' (Plenum Press, New York, 1993).
11. D.W. McKee, *Carbon* **20** (1982) 59–66.
12. G.B. Dunks, *Inorg. Chem.* **23** (1984) 828–37.
13. D.G. Vutetakis and D.R. Skidmore, *J. Electrochem. Soc.* **134** (1987) 3027–35.
14. M.A. Kerzhentsev, M.G. Adamson, Z.R. Ismagilov and Y.S. Chekryshkin, 'Oxidation of organic compounds and CO in some molten salts and catalysts', *in* M. Gaune-Escard (Ed), 'Advances in Molten Salts' (Begell House, New York, 1999), pp. 279–99.
15. W.H.A. Peelen, M. van Driel, K. Hemmes and J.H.W. de Wit, *Electrochim. Acta* **43** (1998) 3313–31.
16. W.R. Smith and R.W. Missen, *Chem. Eng. Educ.* **26** (1979) 122–33.
17. D.H. Coleman and R.E. White, *J. Electrochem. Soc.* **143** (1996) 1781–83.
18. K. Hemmes, W.H.A. Peelen and J.H.W. de Wit, *Electrochim. Acta* **43** (1998) 2025–31.
19. M. Cassir, B. Malinowska, W. Peelen, K. Hemmes and J.H.W. de Wit, *J. Electroanal. Chem.* **433** (1997) 195–205.
20. G.H.J. Broers, M. Schenke and H.J.J. van Ballegoy, Extended Abstract, No. II77, 20th ISE Meeting Druzhba, Bulgaria. Sept. (1977).
21. V.N. Nekrasov, N.M. Barbin and A.P. Pekar, *Russian J. Electrochem.* **33** (1997) 248–54.
22. R. Weewer, K. Hemmes and J.H.W. de Wit, *J. Electrochem. Soc.* **142** (1995) 389–97.